

LA-5703-SR Rev.

Status Report

c.3

UC-21

Reporting Date: November 1974

Issued: February 1975

CIC-14 REPORT COLLECTION  
**REPRODUCTION  
COPY**

Status Report

## Laser Fusion Target Fabrication

30 April 1974

by

R. Jay Fries  
Eugene H. Farnum



**los alamos**  
**scientific laboratory**

of the University of California

LOS ALAMOS, NEW MEXICO 87544



An Affirmative Action/Equal Opportunity Employer

In the interest of prompt distribution, this report was not edited by the Technical Information staff.

This report was prepared as an account of work sponsored by the United States Government. Neither the United States nor the United States Energy Research and Development Administration, nor any of their employees, nor any of their contractors, subcontractors, or their employees, makes any warranty, express or implied, or assumes any legal liability or responsibility for the accuracy, completeness, or usefulness of any information, apparatus, product, or process disclosed, or represents that its use would not infringe privately owned rights.

CONTENTS

ABSTRACT	1
I. INTRODUCTION	1
II. CRYOGENIC TARGETS	3
III. LITHIUM DEUTERIDE/TRITIDE TARGETS	3
A. General	3
B. Spheroidization	3
C. Quality Selection	4
D. Metal Coatings	4
E. D/T Exchange Reaction	4
F. $\text{LiD}_{0.5}\text{T}_{0.5}$ Target Mounting	4
IV. GAS-FILLED TARGETS	5
A. General	5
B. Substrates, Mandrels, and Free-Standing Shells	5
1. Free-Standing Shells	5
2. Nonremovable Mandrels	6
C. Metal Pusher-Shell Deposition	6
1. Chemical Vapor Deposition	6
2. Physical Vapor Deposition and Sputtering	7
3. Electroless Plating	7
4. Electroplating	8
D. Absorber/Ablator Coatings	8
1. Plastic Coatings	8
2. Nonplastic Absorber/Ablator Coatings	9
E. Disk-Type Absorber/Ablator Deposition	9
F. Characterization and Quality Selection	10
1. Size Separation	10
2. Liquid Sink/Float Separation	10
3. Density Separation	11
4. External Pressurization Test	12
5. Microradiography	12
6. Nondestructive Fuel Assay	14
a. X-ray Counting Method	14
b. Elastic Scattering (Van de Graaff) Method	15
c. $D(\gamma, n)$ Reaction Method	15
7. Filling, Permeability and Strength Measurements	16
a. Gas Filling	16
b. Permeability Measurements	17
c. Strength Measurements	18

LOS ALAMOS NATL. LAB. LIBS.



3 9338 00368 0641

CONTENTS (Cont)

G. Target Mounting	18
H. Handling Techniques	19
1. Handling Individual Microspheres	19
2. Storage and Retrieval	20
3. Batch Recovery	20
4. General Remarks Regarding Handling	21
ACKNOWLEDGMENTS	21
REFERENCES	22

LASER FUSION TARGET FABRICATION: A STATUS REPORT  
30 APRIL 1974

by  
R. Jay Fries and Eugene H. Farnum

ABSTRACT

The laser fusion target fabrication effort at Los Alamos Scientific Laboratory has been successful in producing targets of the general design requested by, and with a range of parameters acceptable to, the theoretical designers and to the laser/target interaction physics experimentalists. Many novel techniques for handling and measuring the properties of various types of hollow microballoons have been developed, as described. These various techniques are being documented to provide useful information to other investigators, although we are still far removed from being able to fabricate any type of optimum laser fusion target.

I. INTRODUCTION

In our target fabrication program, we have emphasized the development of hollow, multilayered microspheres that can be filled with high-pressure, noncryogenic DT fuel gas and retain the gas for useful periods of time. In addition, we have developed techniques to fabricate solid LiD and  $\text{LiD}_{0.5}\text{T}_{0.5}$  microspheres and to coat them with high and/or low atomic-number (Z) metals, if desired. Finally, we have devoted a modest effort to the development of cryogenic targets, such as extruded cylindrical rods and rectangular ribbons of solid  $\text{D}_2$ , shells of solid  $\text{D}_2$  or DT frozen out on the inside surface of hollow microspherical containers, and solid microspheres of  $\text{D}_2$  and DT.

The generalized laser fusion target design<sup>1</sup> that has formed the basis of most of our target fabrication development effort is shown schematically in Fig. 1. A central core of high-pressure, gaseous DT fuel is surrounded by a pusher shell of high-Z metal. (Other fuel forms, e.g., solid or liquid DT or  $\text{LiD}_{0.5}\text{T}_{0.5}$  can also be used.) The pusher shell can be either freestanding or deposited on a nonremovable substrate mandrel (such as commercially available glass or metal microballoons). The pusher shell is, in turn, surrounded by an absorber/

ablator shell of a low-density, low-Z material that serves to absorb the energy of the incident laser beam(s) and to provide added compression to the core via ablation and the rocket reaction forces.

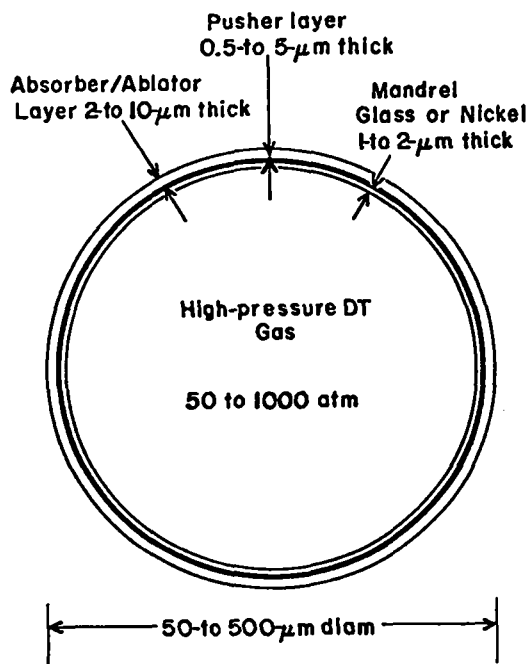


Fig. 1. Schematic of a structured, multilayered laser fusion target.

The laser powers available now and probably for the next several years are such that target diameters from 50 to 500  $\mu\text{m}$  are of interest. Target mass and strength requirements indicate wall thicknesses ranging from 0.5 to 5  $\mu\text{m}$  for the pusher and from 2 to 10  $\mu\text{m}$  for the absorber/ablator layer.

Targets having a flat absorber/ablator disk, rather than the concentric spherical shell, have also been fabricated for use in LASL's one-beam  $\sim 40\text{-J}$ ,  $\sim 40\text{-ps}$ , Nd:Glass laser. This design should improve the symmetry of the energy input into the spherical target from the single laser beam.<sup>2</sup> This so-called ball-and-disk design is shown schematically in Fig. 2 with a glass microballoon as the pusher and a disk-shaped absorber/ablator layer, about four times the target diameter, immediately behind the pusher (i.e., on the side away from the impinging laser beam). A cap of absorber/ablator material is also provided on the front half of the target microsphere. A ball-and-disk target with a gas-filled glass microballoon is shown in Fig. 3. Bare, solid  $\text{LiD}_{0.5}\text{T}_{0.5}$  microspheres (instead of gas-filled microballoons) have also been used in this design.

All our DT-gas-fueled ball-and-disk targets used to date have utilized commercially available glass microballoons as pushers. As a result, we

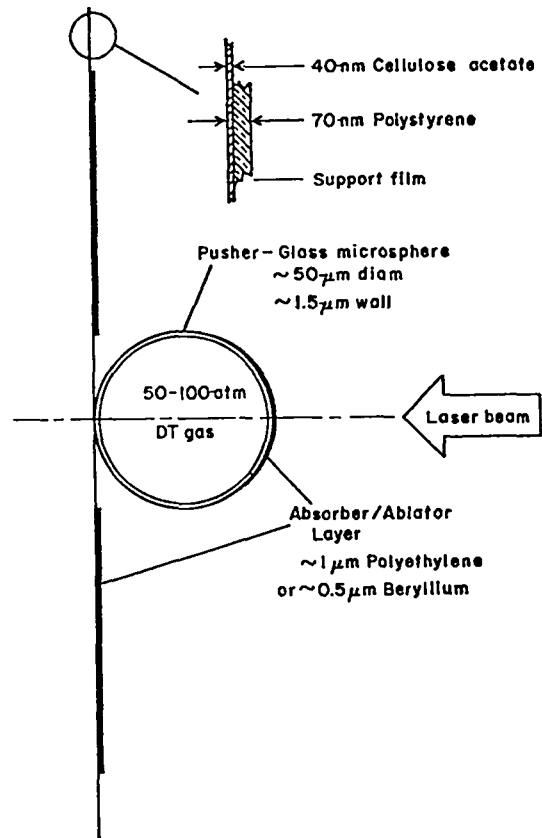


Fig. 2. Schematic of a laser-fusion target of the ball-and-disk design.

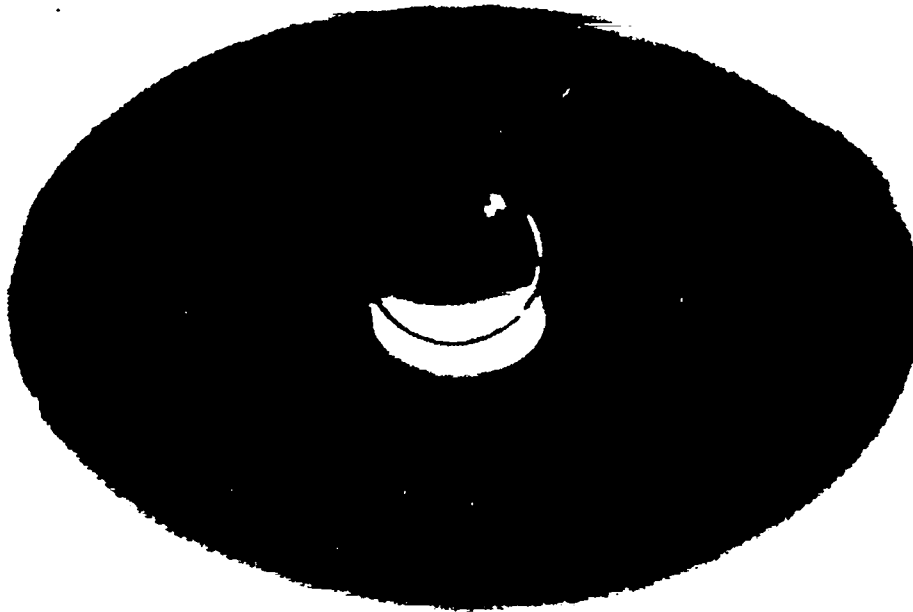


Fig. 3. Ball-and-disk target with a 50- $\mu\text{m}$ -diam glass microballoon as pusher.

have devoted considerable effort to the development of techniques for handling, size separation, quality selection and inspection, and nondestructive fuel assay for the microballoons. In addition, a thin (30- to 110-nm thick) plastic-film support system has been developed and used for both the DT gas and the  $\text{LiD}_{0.5}\text{T}_{0.5}$  solid targets, so as to minimize the extraneous mass in their vicinity.

The process that we have developed for fabricating the solid  $\text{LiD}_{0.5}\text{T}_{0.5}$  microspheres involves crushing and screening LiD stock and spheroidizing these particles. The resulting particles are then reacted with tritium to form  $\text{LiD}_{0.5}\text{T}_{0.5}$  microspheres. We have also devoted considerable effort to the development of characterization and quality selection techniques for LiD microspheres as well as to several metal-coating techniques.

All of these topics are discussed in detail below.

## II. CRYOGENIC TARGETS

We have developed an apparatus to continuously extrude solid 1-mm-diam  $\text{D}_2$  or  $\text{H}_2$  rods suitable for use as laser targets. A modified design has allowed the extrusion of ribbons of rectangular cross-section, about 100- $\mu\text{m}$  thick and 375- $\mu\text{m}$  wide. At slow extrusion rates, the solid  $\text{D}_2$  ribbon curls, but at rates greater than 0.5 mm/s, we are able to obtain a 3-mm-long straight section immediately below the nozzle.

We intend to modify the cylindrical-rod extruding apparatus by adding a pellet cutter and spheroidizing drop tower so that solid  $\text{D}_2$  or DT spheres of 200- $\mu\text{m}$  diameter can be made.

Experiments are being prepared to study the methods and problems of freezing uniform layers of DT ice onto the inside surfaces of hollow spheres. The apparatus for these experiments is being assembled.

An apparatus has been developed for studying the pressure-volume-temperature (PVT) relationships of the solid and liquid phases of the hydrogen isotopes. The apparatus was debugged during initial studies of solid hydrogen. However, some evidence of unexpected phase changes was encountered during these experiments, and our current effort is being devoted to a study of these phenomena.

## III. LITHIUM DEUTERIDE/TRITIDE TARGETS

### A. General

We have developed the processes and techniques to fabricate solid microspheres of LiD and then to convert these to a composition of  $\text{LiD}_{0.5}\text{T}_{0.5}$  by means of the D/T exchange reaction. We are attempting to carry the target fabrication process as far as possible with LiD and then to tritiate the sample so as to minimize the number and types of processing facilities suitable for use with tritium.

The LiD microspheres are made in an argon-flushed dry box. Bulk LiD is first crushed and screened to obtain particles in the desired size range. These particles are then spheroidized by dropping through a resistance-heated drop tower. Following this, the microspheres can be redeuterided, if necessary, to replace any deuterium lost in the spheroidization step. Next, the spheres are selected for quality, are metal-coated if required, and are then converted to  $\text{LiD}_{0.5}\text{T}_{0.5}$  via the D/T exchange reaction. Finally, the microspheres are mounted on an appropriate support and are provided with an ablator coating, if desired, to produce the final target.

### B. Spheroidization

Spheroidization has been the most critical step in the production process. The LiD contracts > 18% on freezing; if the LiD particles are mostly melted during their transit through the drop tower, the resultant spheres will contain large, irregular pores caused by the contraction of the solidifying molten core inside the rigid outside shell that freezes first. This pore formation can be prevented by operating the drop tower at a temperature low enough so that only the surface of the particles is melted.

We are currently using a drop tower consisting of two adjacent, independently heated sections, each  $\sim 9$  cm long. Best results for 40- to 50- $\mu\text{m}$ -diam LiD microspheres are obtained with the upper and lower sections of the drop tower at  $\sim 1065$  and 945 K, respectively (compared to the LiD melting temperature of 995 K). For larger microspheres, the temperature of the upper heater must be increased 10 to 15 K for optimum results. Metallographic examination of cross sections of the 40- to 50- $\mu\text{m}$ -diam microspheres indicates that fewer than 10% of the spherical particles formed in the drop tower under optimized

conditions contain objectionable pores. We have successfully prepared LiD microspheres ranging in size from 44 to 125  $\mu\text{m}$ .

#### C. Quality Selection

We have examined several nondestructive methods of differentiating between porous and nonporous LiD microspheres. Microradiographic inspection with x rays is of limited usefulness because of the very high x-ray transmissivity of the LiD at the x-ray energies available to us ( $\geq 2$  kV). However, the presence of LiOD in the LiD can be clearly seen; and, to the extent that an LiOD coating exists at most interfaces, so can the LiOD-coated cracks and pores in the LiD.

Separation by density, although useful, is somewhat ambiguous because the denser LiOD can mask the presence of pores. In addition, the number of liquids that can be used for separation by floatation is severely restricted because of the high reactivity of the LiD.

The most promising method appears to be optical examination of the microspheres with a laser interferometer, but this technique is still under development and its final capabilities are not yet known.

We use neutron-activation analysis to nondestructively measure the oxygen content of our LiD samples. A 0.2- to 0.5-g sample of LiD powder is placed in a stainless-steel capsule, which is then sealed by welding in a dry box to protect the LiD from hydrolysis during the analysis. This capsule is then neutron-irradiated and analyzed in the usual way.<sup>3</sup> Our LiD stock contains  $\sim 0.2$  wt%  $\text{O}_2$ , while the 40- to 50- $\mu\text{m}$ -diam LiD microspheres contain  $\sim 0.55$  wt%  $\text{O}_2$  after being crushed, screened, and spheroidized in inert-atmosphere dry boxes containing  $\lesssim 10$  ppm of water vapor.

#### D. Metal Coatings

Any metal coatings that we apply to the LiD microspheres should be compatible with the LiD at the 675 K temperature used in the D/T exchange reaction, so that the microspheres can be tritiated after coating. Nickel is a useful coating material from the standpoint of both chemical compatibility and laser/target interaction physics. We have coated several batches of LiD microspheres and non-spheroidized particles with nickel by chemical vapor deposition from  $\text{Ni}(\text{CO})_4$  in a gas-fluidized bed. A  $\sim 1.2$ - $\mu\text{m}$ -thick coating is too permeable to prevent

immediate and violent reaction when the coated LiD microspheres are dropped into water, but a 2.5- $\mu\text{m}$ -thick coating appears to protect LiD microspheres from such reaction and, in addition, to provide protection from long-term reaction with the water vapor present in ambient laboratory air. (However, a 2.5- $\mu\text{m}$ -thick nickel coating on irregular, nonspheroidized LiD particles is not observably better than the 1.2- $\mu\text{m}$  coating, providing only slight protection.) These coatings do not observably affect the rate of the D/T exchange reaction, nor is there any evidence of a reaction between the coating and the LiD substrate.

#### E. D/T Exchange Reaction

The D/T exchange reaction is carried out in an apparatus consisting of a cylindrical, water-cooled external pressure vessel containing at its center a smaller, open-ended tube. This tube can be heated to  $\sim 675$  K and contains the sample to be exchanged. The apparatus is charged with a tritium/deuterium gas mixture at about 1 atm. The initial gas composition is calculated on the basis of the mass and composition of the LiD to be exchanged so as to give an equilibrium composition in the solid of about  $\text{LiD}_{0.5}\text{T}_{0.5}$ . The concentric hot-and-cold design allows the circulation and mixing of the gases by means of thermal convection. The progress of the reaction was followed during initial hydrogen-deuterium exchange runs by monitoring the gas composition with a small, residual-gas-analyzer mass spectrometer. These experiments indicated that equilibrium was attained in less than 24 h under our experimental conditions. On this basis, the D/T exchange reactions were run for 24 h. Calculation of the final solid composition based on the solid mass, the amount of gas used, and its composition before and after the run confirm that equilibrium was attained.

#### F. $\text{LiD}_{0.5}\text{T}_{0.5}$ Target Mounting

We have mounted bare, 40- to 50- $\mu\text{m}$ -diameter  $\text{LiD}_{0.5}\text{T}_{0.5}$  microspheres as targets of the ball-and-disk design, on 100-nm-thick plastic support films, using a 200- $\mu\text{m}$ -diam disk of polyethylene, 1- $\mu\text{m}$ -thick, as the absorber/ablator disk. This polyethylene disk was vapor-deposited through a mask (as described below) onto the plastic support film using a glass microballoon as a "stand-in" for the  $\text{LiD}_{0.5}\text{T}_{0.5}$  microsphere. The glass microballoon was then carefully removed and replaced with a  $\text{LiD}_{0.5}\text{T}_{0.5}$



microsphere, thinly coated with oil to protect it from hydrolysis. Also, the surface-tension forces of the oil hold the microsphere in place on the film. In addition, we have mounted oil-coated  $\text{LiD}_{0.5}\text{T}_{0.5}$  microspheres by attaching them to a fine glass fiber ( $\sim 2\text{-}\mu\text{m}$ -diam) that was stretched across the aperture of the metal target holder and cemented in place with polystyrene. The surface-tension forces of the oil hold the microsphere in place on the fiber.

#### IV. GAS-FILLED TARGETS

##### A. General

As mentioned above, the major fraction of our target fabrication efforts has been devoted to hollow, multilayered microspheres filled with high-pressure DT gas (Fig. 1). This assembly must be strong enough to withstand the hoop stresses resulting from the high pressure of the fuel gas at room temperature, so that we do not have to provide a cryogenic holder in the target chamber. (However, we do not object to cryogenic storage of the fueled target prior to mounting in the target chamber to minimize permeation losses of the fuel gas.)

The DT fuel gas is loaded into the targets by diffusion through the wall at elevated temperatures. Because permeability is an exponential function of temperature, most of our targets can be designed to be filled in several hours at temperatures of 475 to 775 K and still retain the gas for useful periods of time at room temperature.

The physics of laser target fusion indicate that the initial DT fuel gas be as dense as possible. As a result, we have emphasized the development of high-strength pusher and absorber/ablator shells.

##### B. Substrates, Mandrels, and Free-Standing Shells

Free-standing pusher shells are desirable to minimize the nonfuel mass of the target and thus to maximize yield efficiencies. Unfortunately, thin-walled microballoons of sufficiently high strength and quality are not available commercially, whereas glass and metal microballoons are available that are suitable for use as mandrels onto which pusher shells of the desired properties can be deposited. Therefore, we are developing the capabilities of depositing high-strength, metal pusher shells onto nonremovable mandrels for use as first-generation targets, in spite of their higher total mass.

Simultaneously, we are trying to develop techniques to deposit free-standing, high-strength pusher shells.

1. Free-Standing Shells. Two possible methods of fabricating free-standing spherical shells are:

(a) the deposition of the shell onto a mandrel that is subsequently removed, and (b) the blowing of bubbles from molten metal, which then solidify into hollow spheres.

All commercially available, hollow microballoons that we are familiar with are made by the second method. Examination of these commercial products quickly led us to conclude that the production of high-quality microballoons by this method is very difficult. The yield of spherical, nonporous microballoons of uniform wall thickness is very small, even when the manufacturers, at our request, try to optimize the process. In addition, a major development effort is required to adapt the process to produce microballoons of different composition or from other metals.

The above considerations suggested that we concentrate on the first method of producing free-standing microballoons, i.e., the deposition onto, and subsequent removal of, a mandrel. As a result, we have deposited nickel onto carbon mandrels and then attempted to diffuse the carbon out through the nickel wall by heat-treating in hydrogen. Unfortunately, a heat-treat temperature of  $\sim 1275$  K was required to obtain a carbon-hydrogen reaction rate that was not prohibitively slow. Even at that temperature, more than 60 h were required to remove a  $195\text{-}\mu\text{m}$ -diam solid carbon mandrel through a  $3\text{-}\mu\text{m}$ -thick nickel wall. Unfortunately, the nickel wall was destroyed in the process, being puckered and porous at the conclusion of the heat-treatment. However, we expect that the method will work without destroying the shell for metals having higher metal-carbon eutectic temperatures; additional experiments are therefore planned with molybdenum, rhenium, and titanium metal shells. High-quality solid carbon spheres are available for use as mandrels and it is likely that porous carbon spheres (or possibly hollow spheres) will be available that would minimize the quantity of carbon to be removed.

Another approach that we are pursuing is the formation of porous metal coatings on easily volatilized spherical mandrels, such as paraffin. These

assemblies will then be heat-treated, first to remove the mandrel and then to sinter the metal shell.

2. Nonremovable Mandrels. We have used commercially available microballoons of a nickel alloy and of glass as nonremovable mandrels onto which to deposit metal pusher shells. The nickel-alloy microballoons are Solacells obtained from the Solar Division of International Harvester, with a composition by weight of  $\sim 60\%$  nickel,  $20\%$  manganese,  $2.5\%$  silicon,  $1.5\%$  each iron and boron, and trace quantities of numerous other metals. (N.B. All composition data reported are in weight percent). The Solacells are available in sizes from  $75\ \mu\text{m}$  to greater than  $500\text{-}\mu\text{m}$  diameter, with wall thicknesses of  $0.8$  to  $2.5\ \mu\text{m}$ . Our experience indicates a softening temperature of  $\sim 1000\ \text{K}$  for these.

Glass microballoons have been obtained from Emerson and Cuming Company (Eccospheres) and from Minnesota Mining and Manufacturing Company (3M microballoons). Eccospheres are available in many different grades, but we have examined only two of these in detail: (1) the IG-101 grade, a soft soda glass ( $\sim 78\% \text{SiO}_2$ ,  $3\% \text{B}_2\text{O}_3$ ,  $19\% \text{Na}_2\text{O}$ ) and (2) the SI grade, a borosilicate glass ( $\sim 92\% \text{SiO}_2$ ,  $2.5\% \text{B}_2\text{O}_3$ ,  $2.5\% \text{Na}_2\text{O}$ , balance unknown) that is obtained by acid-leaching the IG-101 grade. The softening temperatures of these Eccospheres are reported to be  $725$  and  $1275\ \text{K}$  for the IG-101 and the SI grades, respectively. The size of the Eccospheres ranges from  $< 40\ \mu\text{m}$  through  $175$  to  $200\ \mu\text{m}$ , with wall thicknesses of  $1$  to  $2\ \mu\text{m}$ .

Many types of 3M glass microballoons are available, but we have used primarily the B40A type to date. This type is made from a soda-lime glass ( $\sim 80\% \text{SiO}_2$ ,  $11\% \text{Na}_2\text{O}$ ,  $6.5\% \text{CaO}$ ,  $2.5\% \text{B}_2\text{O}_3$ ) in about the same size range as the Eccospheres and has a softening temperature of  $\sim 825\ \text{K}$ . The wall thickness ranges from about  $1$  to  $3\ \mu\text{m}$ . Other 3M types have thinner walls, and we are beginning to evaluate some of these also.

The Eccospheres contain residual  $\text{N}_2$  and  $\text{CO}_2$  gases at pressures of  $\sim 50$  and  $100$  torr, respectively, as well as traces of  $\text{H}_2\text{O}$ ,  $\text{O}_2$ , and other gases. (These are presumably decomposition products of the urea used as the blowing agent in the manufacturing process.) The 3M microballoons contain residual  $\text{SO}_2$  and  $\text{N}_2$  gases at pressures estimated to be at most  $290$  and  $10$  torr, respectively, as well as smaller

quantities of oxygen and other gases. Heat-treatment in a hydrogen-fluidized bed for  $20\ \text{h}$  at  $\sim 975\ \text{K}$  removed essentially all the  $\text{CO}_2$  and  $\sim 20\%$  of the nitrogen from the SI Eccospheres and all the  $\text{SO}_2$  from the 3M microballoons. A thin coating of nickel ( $0.2$  to  $0.5\text{-}\mu\text{m}$  thick) on the 3M microballoons effectively prevented agglomeration during this heat-treatment which is carried out some  $150\ \text{K}$  above the softening temperature of these microballoons. The larger ( $\sim 100\text{-}\mu\text{m}$  diam) 3M glass microballoons tended to wrinkle and to collapse under these heat-treat conditions, but this effect was largely eliminated when we reduced the hydrogen pressure to  $\sim 200$  torr from our usual  $580$  torr--the normal atmospheric pressure at Los Alamos.

Additional experiments have shown that the B40A glass microballoons can be outgassed effectively at a temperature of  $675\ \text{K}$ , well below their softening temperature. This property eliminates the need for a nickel coating and also the wrinkling and shriveling of the larger microballoons.

We have measured the permeabilities of these mandrels, as discussed below, and have also established the conditions for gas filling. The Solacells and the SI Eccospheres can be filled to the  $\text{D}_2$  or  $\text{DT}$  gas supply pressure in less than three hours at  $575\ \text{K}$ . In contrast, present data indicate that the 3M microballoons can be filled to only  $\sim 50\%$  of the supply pressure in  $\sim 60\ \text{h}$  at  $675$  to  $700\ \text{K}$ , and that the permeability of IG-101 Eccospheres is so low that barely measurable amounts of gas permeate through the wall in  $60\ \text{h}$  at the same temperature.

### C. Metal Pusher-Shell Deposition

1. Chemical Vapor Deposition. We have pursued several different methods of metal pusher-shell deposition. Chemical vapor deposition (CVD), which involves the deposition of the desired metal by means of thermal decomposition or chemical reduction of appropriate metal-containing gases, has been one of the more useful methods. A gas-fluidized bed of the particles to be coated is usually used for the CVD process, which tends to minimize agglomeration and sticking of the very light microspheres during coating. We have developed CVD methods to deposit nickel [thermal decomposition of  $\text{Ni}(\text{CO})_4$  at  $\sim 375\ \text{K}$ ], molybdenum [chemical reduction of  $\text{MoF}_6$  with hydrogen at  $\sim 875\ \text{K}$  or thermal decomposition of  $\text{Mo}(\text{CO})_6$  at  $525$  to  $675\ \text{K}$ ], tungsten (chemical reduction of  $\text{WF}_6$

with hydrogen at  $\sim 725$  K), and rhenium (chemical reduction of  $\text{ReF}_5$  with hydrogen at 525 K). These CVD coatings can be applied to Solacell or glass microballoon mandrels, as well as to carbon spheres. Good-quality coatings can be obtained at least as thin as  $\sim 0.1 \mu\text{m}$  and up to thicknesses substantially greater than  $10 \mu\text{m}$ .

We are trying to improve interparticle coating uniformity for very thin coatings by means of appropriate substrate pretreatment and fluid-bed design. We are also trying to increase the strength of the CVD coatings by controlling the morphology of the deposit with techniques such as mechanical abrasion during coating and by interrupted coatings.

Finally, we are investigating techniques that would allow very small quantities of preselected microspheres (as few as 50 to 100 particles) to be coated and quantitatively recovered. A small, liquid fluidized bed was developed for this purpose and successfully used for nickel-coating from  $\text{Ni}(\text{CO})_4$ . However, scanning electron microscopy showed the coating to consist of a relatively porous agglomeration of very small nickel spheroids. This type of coating would probably be acceptable as a high-Z layer, but it would certainly be useless as a gas container. Gas-fluidized beds will be tried next, mixing the spheres of interest with others of a different size to form a particle bed large enough for coating, and then using precision screening to recover the spheres of interest from the remainder of the bed.

Other potentially useful pusher materials for which CVD techniques are under development include titanium (because of its high strength-to-weight ratio) and alloys of W:Re and W:Mo because of their high strengths. (Titanium is a questionable material because it may be difficult to permeate useful quantities of DT fuel gas through the wall; we are therefore particularly anxious to obtain samples of this material to test.)

## 2. Physical Vapor Deposition and Sputtering.

Physical vapor deposition (PVD) has also been used to apply metal coatings, but primarily for very thin coatings. PVD involves the thermal vaporization of the desired metal from a hot filament (or crucible) in vacuum and its subsequent deposition onto the cold substrate. The metal vapor travels only in line-of-sight directions from the vaporization

source and condenses as soon as it encounters a cool surface. As a result, to obtain uniform coatings on three-dimensional substrates, they must be kept in motion continuously, e.g., by vibrating or tumbling in a barrel. We found it very difficult to keep the very small, lightweight substrate particles we must work with in uniform motion, and coating uniformity therefore is generally rather poor. In addition, the thicker coatings require relatively long coating times, which accentuate the coating-uniformity problem and give rise to interparticle-agglomeration problems, also. As a result, and because of the generally good results obtained with the CVD methods, we have not devoted much effort to PVD for high-Z pusher shells. However, we have successfully applied very thin coatings of PVD nickel on glass microballoons by using vibratory table agitation and of PVD chromium on glass microballoons by using a barrel tumbler. In both cases, the coated glass microballoons were used as substrates for electroless plating experiments discussed in the next section. In addition, we have deposited absorber/ablator layers of beryllium and polyethylene by using PVD techniques, as discussed below.

We have acquired a Sloan Sputtergun that sputters metal atoms from an appropriate cathode when bombarded with ions in an argon glow discharge. The sputtered metal atoms also travel in line-of-sight directions, and the requirements of substrate agitation are therefore the same as for PVD. However, the sputtergun offers the possibility of depositing multicomponent metal mixtures, which could lead to the use of complex high-strength alloys as pusher shells. To date, this sputtergun has only been used for beryllium deposition (discussed below), but deposition of other metals and alloys is planned.

3. Electroless Plating. Electroless plating involves the chemical reduction of appropriate metal ions in an aqueous solution and the subsequent deposition of the metal atoms onto solid mandrels that are dispersed in the solution. Techniques have been developed for electroless plating of nickel, nickel/cobalt alloys, and copper on all of our substrate types (i.e., glass microballoons, Solacells, and carbon microspheres). However, the glass microballoons must be given a preliminary flash metal coating prior to the electroless plating. The major problem has been agglomeration of substrate particles (which

float on the surface of the plating bath), but appropriate agitation and stirring techniques have been developed to allow yields of more than 80% of unagglomerated, coated particles at a coating thickness of 5 to 10  $\mu\text{m}$ . We are able to electroless-plate coatings to thicknesses ranging from  $< 1 \mu\text{m}$  to  $> 20 \mu\text{m}$ .

Electroless nickel coatings deposited with hypophosphite and with dimethylamine borane (DMAB) reducing agents have been prepared so that the strengths of these two coatings can be compared, because published data<sup>4</sup> indicate that the resulting Ni(+B) deposits are harder (and therefore stronger?) than the Ni(+P) deposits. Another paper<sup>5</sup> reported that the strength of Ni(+B) deposits could be increased by heat-treating, and we therefore want to evaluate this effect for both alloys. Similarly, the nickel/cobalt alloys have been prepared so that the strengthening effect of the cobalt additions can be evaluated.

4. Electroplating. The potentially higher strength of electroplated metal coatings has prompted us to devote some effort to developing techniques for electroplating the small spherical mandrels. The primary problem, of course, is making electrical contact to the microspheres while preventing them from sticking to the electrode. We have progressed to the point where we can electroplate 250- $\mu\text{m}$ -diam Solacells with 2  $\mu\text{m}$  of either copper or nickel to yield  $\sim 20$  to 30% of useful particles. We plan to optimize the techniques of plating with copper (which is easy) and then to plate some high-strength nickel deposits, as well as some high-strength alloys.

#### D. Absorber/Ablator Coatings

Two general types of low-Z, low-density absorber/ablator materials have been under development for uniformly coating the pusher shells. These are plastic, e.g., parylene (polyparaxylene, prepared by a Union Carbide Corporation licensed process) and polyethylene that offer essentially no strength to the target assembly; and coatings of beryllium, boron, or carbon that may substantially strengthen the pusher-ablator assembly. We want to be able to load the fuel gas into the targets by diffusion through the complete target assembly with the absorber/ablator coating already in place. This will probably be possible for all the absorber/ablator coatings discussed here except the polyethylene.

1. Plastic Coatings. Parylene offers several advantages, including its high-temperature capabilities (stable to at least 475 K) and its ability to coat uniformly in a non-line-of-sight manner. As a result, considerable effort has been devoted to trying to acquire a parylene coating capability. Work has been carried out in coaters of Union Carbide design, as well as in a small all-glass unit of local design. However, we have not yet been able to avoid bonding the particles to each other and to the walls of the coater. As a result of these problems, and of difficulties in obtaining suitable license arrangements with Union Carbide, we are no longer actively working on the parylene process. (However, if a successful license agreement can be worked out that gives us access to the skills and knowledge of Union Carbide, we will resume this work.)

We have developed another process that results in a polymer of paraxylene, but one that is substantially more cross-linked than parylene. We are now using a technique originally developed for vinyl pyridine deposition, in which the monomer vapor is passed through an argon glow discharge at about 200 torr.<sup>6</sup> This activated monomer then attaches to active sites on the substrate or to active sites on previously deposited monomers, polymerizing as it deposits. Our process involves levitation of the microspheres between two metal plates across which we apply  $\sim 300$  V at 10 kHz. The activated monomer is then directed into the space between the two plates so as to coat the levitated substrate particles. Preliminary experiments indicate that acceptable coatings can thus be obtained on both Solacells and glass microspheres if paraxylene is used as the monomer.

Other plastic coating techniques such as suspension-polymerization and solvent-casting have been investigated with some tantalizing hints of success but no clear-cut demonstration of practicability. Here again, the primary problem is one of agglomeration of our very small, light-weight substrates.

Techniques for PVD of a low-molecular-weight, low-melting-temperature polyethylene have recently been developed for deposition of disk-type ablators. In this method, the polyethylene is boiled in an electrically heated crucible to produce an effusing vapor beam that is then used for PVD onto an appropriate substrate. The success of this method for deposition of flat disk ablators prompted us to try

it also for applying uniform coatings to microspheres. The microspheres were agitated on a vibratory table, and the crucible was designed to obtain a downward-effusing vapor beam. Serious particle agglomeration was encountered that has not yet been eliminated successfully. We plan next to try electrostatic particle levitation with a horizontally directed PVD polyethylene source.

2. Nonplastic Absorber/Ablator Coatings. We have developed the techniques for CVD of boron onto glass-microsphere or Solacell substrates by means of the thermal decomposition of diborane at 575 to 875 K. Rather dilute concentrations of diborane were used initially. As a result, the deposition rate was too slow to obtain boron layers of micron thicknesses in reasonable times. A much more concentrated solution of diborane (15%) in argon has been obtained and new boron coating runs are in progress.

A method of sputtering beryllium uniformly onto glass microballoons that are agitated on a vibrating table under the sputtergun has been developed. The addition of a water-cooled grid electrode between the sputtergun and the substrate, and pretreatment of the glass microballoons in acetone (which seems to minimize agglomeration at least for the SI Eccospheres) are both required to allow us to obtain coatings of uniform thickness. Beryllium coatings about 1  $\mu\text{m}$  thick have been deposited, and metallographic examination indicates high-quality coatings of uniform thickness on  $\sim 5\%$  of the particles. Additional experiments are planned to try for thicker coatings and to improve the yield. In addition, similar beryllium coating runs have been made in a hot-filament PVD apparatus where beryllium is melted onto a tungsten filament and physically vapor-deposited therefrom. Here, we obtain good coating uniformity and reasonable yields but it is difficult to obtain 1- or 2- $\mu\text{m}$ -thick coatings because of our beryllium wire-feed arrangement. A modification of the apparatus is under way, which should allow us to obtain thicker coatings.

Several attempts have been made to deposit a pyrocarbon coating onto previously tungsten-coated Solacells by the pyrolysis of acetylene in a fluidized bed. The tungsten coating was an attempt to provide a substrate that would survive the 1275 K and higher bed temperatures required for good pyrocarbon deposition.<sup>7</sup> Unfortunately, the tungsten

coating did not prevent agglomeration and subsequent "freezing" of the fluid bed. A very poor, sooty carbon deposit was obtained in one run at 1175 K during which the central portion of the bed remained fluid, but this coating was too weak to be of interest. We intend to repeat these experiments as soon as we have a substrate that will withstand the high-temperature deposition conditions.

One of the big questions that must be answered about these boron, beryllium, and pyrocarbon absorber/ablator layers concerns their permeability to our fuel gas. The scant literature data indicate that beryllium is relatively impermeable to hydrogen,<sup>8</sup> and discussions with people using pyrocarbon as nuclear-reactor-fuel particle coatings suggest that at least some forms of pyrocarbon are also likely to be rather impermeable.<sup>9</sup> However, no one has had any experience with layers as thin as those we require or, except for the pyrocarbon, with the particular morphologies we will encounter. Thus, the question remains and can only be answered by experimentally measuring the permeability of some appropriate coatings, which we are doing.

#### E. Disk-Type Absorber/Ablator Deposition

Recently we have fabricated targets with the thin disk-type absorber/ablator described above (see Fig. 2). We have developed a PVD method to deposit this absorber/ablator disk through an appropriate mask onto premounted targets. The  $\sim 50\text{-}\mu\text{m}$ -diam, gas-filled targets are mounted on the plastic support film (as discussed below), and a thin (50-to 75- $\mu\text{m}$ -thick) mask containing an appropriate hole is clamped in front of the target so that this hole is concentric with the target sphere. The assembly is then placed in the appropriate PVD apparatus and the absorber/ablator is vapor-deposited through the mask so as to coat the front surface of the sphere, as well as the support film, out to the diameter of the hole in the mask.

Both polyethylene and beryllium have been used as absorber/ablator layers, with thicknesses of 1 and 0.5  $\mu\text{m}$ , respectively. The polyethylene is vaporized by boiling in a crucible as has been described in the preceding section. The target assembly is supported  $\sim 5$  cm above the crucible mouth, and deposition times of  $\sim 20$  min are used to obtain a layer 1- $\mu\text{m}$  thick. Because the deposition process takes place at a relatively low temperature (crucible

temperature, < 750 K), it is not necessary to cool the target assembly. We have not been able to detect any changes in either the target or the support film as a result of depositing polyethylene under the above conditions.

The beryllium is deposited from a hot tungsten filament onto which beryllium wire is melted. Because this process requires relatively high temperatures (filament temperature, ~ 1700 K), the target assembly is located on a water-cooled holder, 15 to 20 cm below the filament. In addition, a cyclic deposition process is used, with deposition times of 30 to 60 s followed by cooling times of 5 min. (A total of five 30-s deposition cycles will deposit a 0.5- $\mu$ m-thick layer of beryllium.) In this case, the plastic support film is slightly deformed in the area covered by the beryllium. This hot-filament technique has also been used to deposit layers of nickel or gold on the backs of the beryllium- or polyethylene-coated target/film assemblies.

#### F. Characterization and Quality Selection

A large portion of our total target fabrication effort has been devoted to the development of techniques to characterize the mandrels, pusher shells, and absorber/ablator coatings, and to separate good targets from undesirable ones, preferably in batch quantities. These techniques include size selection (both by diameter and wall thickness), removal of porous targets by sink-or-float methods, crushing of aspherical and nonuniform-wall spheres by external pressure, and final quality verification by x-ray microradiography. In addition, techniques have been developed to measure gas permeabilities and bursting strengths and to nondestructively measure the amount of deuterium and/or tritium fuel contained within individual target microspheres.

1. Size Separation. The small size and very light weight of our microspheres accentuate interparticle agglomeration resulting from electrostatic and surface forces. Consequently, the primary problem encountered in size separation is that of breaking up clumps of particles and preventing their re-agglomeration. Wet screening has proven to be an effective method, and two such methods have been developed. One method employs essentially conventional screening techniques with mechanical agitation of the screen stack, but provides in addition a small flow of water down through the stack of

screens. This method can be used with the standard 20-cm-diam screens and has a relatively high throughput.

A second, rather unconventional, method (known as inverted screening) has been developed in which the screening operation is carried out completely under liquid (ethanol being most frequently used). Because the bouyant force on the microballoons predominates, they try to move upwards to the liquid surface. Thus, the screens are arranged upside-down with the screen containing the largest holes on the bottom and that containing the smallest holes on the top of the stack. The sample to be sized is placed under the bottom-most screen. The particles are agitated by carrying out the entire operation in an ultrasonically vibrated bath. The size-separated fractions in our ultrasonic tank are recovered best if the small, 7.62-cm-diam screens are used. Thus, the throughput is substantially lower than that of the other method, but the quality of size separation is considerably better. Another advantage accrues to the second method because any grossly porous microballoons fill with liquid and do not float, thus being removed at the outset.

2. Liquid Sink/Float Separations. Sometimes it is desirable to remove the microballoons containing relatively gross porosity from a large batch. A very effective means is the liquid sink/float technique which involves using a separatory funnel (that can be evacuated) to contain the mixture of liquid and particles. Alternately evacuating the vessel and bringing it back up to atmospheric pressure facilitates penetration of the liquid into the smaller pores because the surface tension of the liquid tends toward zero when it boils (as it will even at room temperature if the pressure is sufficiently reduced). In addition, the boiling action tends to break up agglomerates. Finally, spheres containing small holes, but not yet full of liquid, will be partially evacuated when the vessel is evacuated. Then, when the vessel is depressurized to ambient, the differential pressure will tend to force the liquid into the partially evacuated spheres. By using the separatory funnel the sunken spheres can be drawn off conveniently through the stopcock in the bottom of the vessel. The liquid to be used must, of course, be denser than the sound microballoons. We frequently use n-pentane as the liquid in this procedure.

3. Density Separation. The object here is to separate closely sized microballoons according to density, which in fact corresponds to a separation according to average wall thickness. Because the apparent density of our microballoons can be as low as  $0.05 \text{ g/cm}^3$ , liquid sink/float methods are not applicable because appropriate low-density liquids do not exist. Two gas-floatation methods have been developed therefore, one employing gas-phase elutriation in flowing argon, the other employing static  $\text{SF}_6$  gas at high pressures.

In the argon elutriation method, a fluid-bed type column is set up, is loaded with a charge of previously sized particles, and the charge is fluidized with flowing argon gas. The gas flow can be adjusted so that the lighter particles are carried out the top of the bed and collected in an appropriate vessel, while the heavier particles stay behind. This method (used only on glass microballoons to date) has been quite effective in making a relatively coarse density separation such as separating empty microballoons from those containing smaller spheres inside (i.e., the "pregnant" ones). However, a considerable development effort would be required to adapt the method for separating particles having small differences in density (and thus wall thickness). In view of the good results obtained with the second, static-gas method, this effort is neither necessary nor justified. Elutriation, however, has the advantages of simplicity and a rather high throughput.

The static method employs high-pressure  $\text{SF}_6$  gas in the apparatus depicted in Fig. 4. The density of the  $\text{SF}_6$  can be adjusted from  $< 0.01 \text{ g/cm}^3$  to a maximum of  $\sim 0.7 \text{ g/cm}^3$  by controlling its pressure, so that microballoons of lesser density within this range can be floated. The apparatus consists of a 2.5-cm-i.d. cylindrical metal vessel oriented vertically and provided with glass hemispherical end caps to permit observation of the separation process. A conical collector vessel with a mouth diameter of 2 cm is located on the axis of the cylinder with its mouth facing upwards, just below the upper glass cap. This allows the lower density particles to float upwards past the conical collector and to collect at the top of the hemispherical end cap. When the gas density is reduced by lowering the pressure, the microballoons collected in the top

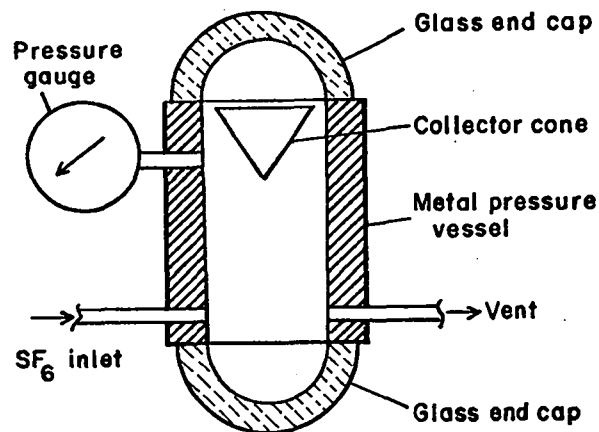


Fig. 4. Schematic of high-pressure-gas density separator.

hemisphere tend to fall straight down and to drop into the conical collector.

Sulfur hexafluoride was chosen because of its high molecular weight, low critical temperature (319 K), and its inertness and nontoxicity. The entire apparatus is mounted in a drying oven and operated at  $\sim 330 \text{ K}$  to prevent condensation of the  $\text{SF}_6$ . The vessel has been operated successfully at 40 atm, which corresponds to a density approaching  $0.7 \text{ g/cm}^3$ . The one difficulty encountered with this apparatus is the proclivity of the microballoons (particularly the glass ones) to agglomerate. This tendency is minimized by vibrating the pressure vessel periodically with a vibratory engraving tool. We are evaluating appropriate pretreatment of the microballoons (e.g., a very thin metal coating) as well as antistatic treatment of the pressure vessel (metal-coating the glass end caps and including a radioactive source in the pressure vessel) to prevent agglomeration. However, even without these refinements, the method is useful to separate the microspheres according to wall thickness.

One further advantage of this  $\text{SF}_6$  method is its ability to separate the porous microballoons from those not containing any porosity. The  $\text{SF}_6$  gas should be able to penetrate through very small micropores so that the effective density of any porous microballoon will be that of its wall material. Therefore, the porous microballoons can be eliminated by collecting only the floating spheres. Also, any spheres that are broken by the applied external pressure will automatically be separated from the sound ones.

4. External Pressurization Test. The objective of this procedure, commonly known as the "crunch test", is to destroy microballoons that are aspherical, contain nonuniform walls, or contain defects in the walls. A perfect sphere having a uniform thin wall (i.e., wall thickness less than 10% of the radius) will fail by elastic buckling at an applied external pressure,  $P_{ext}$ , given by

$$P_{ext} \approx 1.46 E \left( \frac{t}{D} \right)^2,$$

where  $E$  is Young's modulus of the wall material,  $t$  is the wall thickness, and  $D$  is the mean diameter.<sup>10</sup> Any deviation from a spherical shape or from a uniform wall will substantially decrease the pressure at which elastic buckling occurs. Possibly, our smaller microballoons (e.g.,  $\sim 50\text{-}\mu\text{m}$  diam) will fail as a result of excessive compressive hoop stresses (given by  $S_c = P_{ext} D/4t$  where  $S_c$  is the compressive hoop stress and the other symbols are as defined above).<sup>10</sup> However, aspherical particles and/or those with nonuniform walls should still fail at pressures substantially less than those predicted by the formula for good spheres.

In practice, the method is applied by first determining experimentally the relationship between applied pressure and number of spheres surviving, using only a small portion of the batch to be tested. A pressure is then chosen that will give a reasonable balance between number and quality of survivors, e.g., 10 to 20% spheres surviving, and the remainder of the batch of spheres is then subjected to that pressure.

A typical set of data is plotted in Fig. 5. These data were obtained for a batch of SI Eccospheres that had been heat-treated, sized to  $\sim 50\ \mu\text{m}$  diameter, and floated in 20 atm of  $\text{SF}_6$  (corresponding to a density of  $\sim 0.16\ \text{g/cm}^3$ ). In this case, an applied external pressure of 200 atm breaks all but 20% of the spheres, and it would probably be a good pressure at which to crunch the remainder of the batch.

Note that after this crunch test, the good spheres must be separated from those that were broken in the test. Inverted screening in an ethanol bath is particularly effective for this separation but the high-pressure gas sink/float test can also be used.

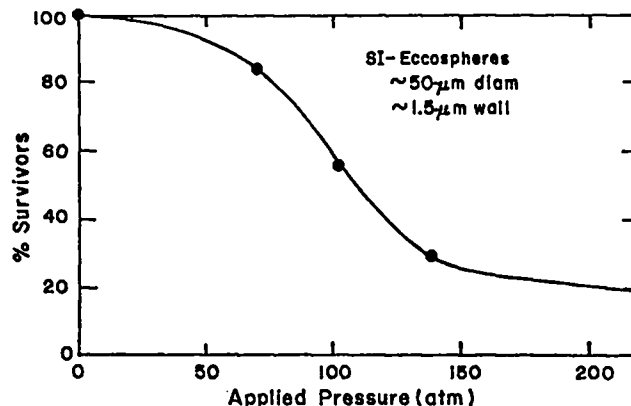


Fig. 5. Typical crunch-test results for SI-Eccosphere glass microballoons.

5. Microradiography. Microradiography has been developed for use as a nondestructive final inspection technique to verify the sphericity, wall-thickness uniformity, and absence of other flaws and defects in the target microspheres.

The microballoon to be radiographed is placed on a sheet of 4- $\mu\text{m}$ -thick Mylar film, and a microdrop of oil is then placed under the balloon. The surface tension of the oil film effectively immobilizes the microsphere, eliminating interaction between nearby neighbors. This technique facilitates identification and retrieval of individual microspheres so that the information obtained from the radiograph can be utilized in selecting or eliminating particular targets. This mounting technique is described in detail in Section F-2, below.

The Mylar film is mounted in a holder that contains appropriate O-rings and evacuation ports so that a vacuum can be used to pull the Mylar film into intimate contact with the emulsion side of a Kodak high-resolution spectrographic plate. This assembly is then placed  $\sim 90\ \text{cm}$  below the x-ray generator which has a 0.5-mm-square focal spot size. The air in the x-ray path can be replaced with helium if desired. A radiograph is then taken by using x-ray energies and exposure times previously determined to give optimum resolution.

With this procedure, radiographic images can be obtained that have a resolution limited only by the grain size in the developed image, i.e., about  $\pm 0.25\ \mu\text{m}$ . The diameters and wall thicknesses of the targets are measured from the radiograph with a



metallographic type microscope equipped with a calibrated filar ocular. A series of verification experiments was run in which measurements were made on metallographic cross sections prepared of previously radiographed and measured glass microballoons and Solacells. The microspheres were immobilized so that the metallographic cross sections could be obtained at the equatorial planes viewed in the radiographs. Good agreement was obtained between the two sets of measurements indicating that the radiographic images were being correctly interpreted and measured. Microradiographs of various good and defective microballoons are shown in Fig. 6.

The minimum x-ray energy available in the apparatus described above is  $\sim 10$  kV (peak), which is too high to produce good images of thin, low-Z, low-density layers such as beryllium and plastic.

As a result, we have modified a vacuum electron-beam vapor-deposition apparatus so that it can be used as a source of low-energy x-rays (1 to 10 kV peak). We are obtaining very good results with this unit, as illustrated by Fig. 7 which shows glass microballoons coated with plastic.

We are also developing methods of mounting the microballoons so that radiographs of three or four different equatorial planes can be obtained. This will allow complete inspection of all surfaces of the microballoons. In addition, we are looking into methods of increasing the resolution of the microradiographic method to the  $\pm 0.1\text{-}\mu\text{m}$  level and at other methods, such as interferometry, that might allow even higher resolution.

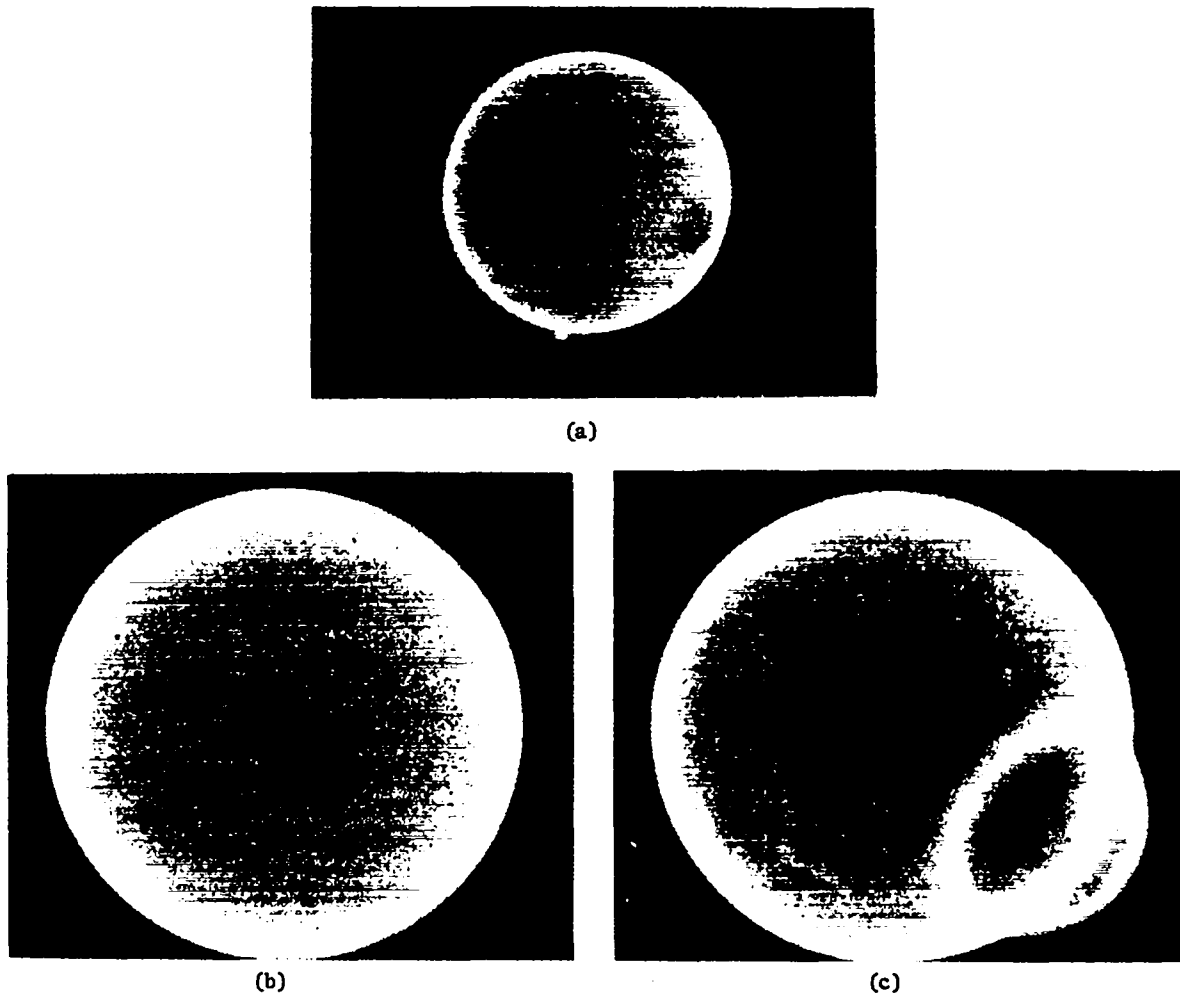
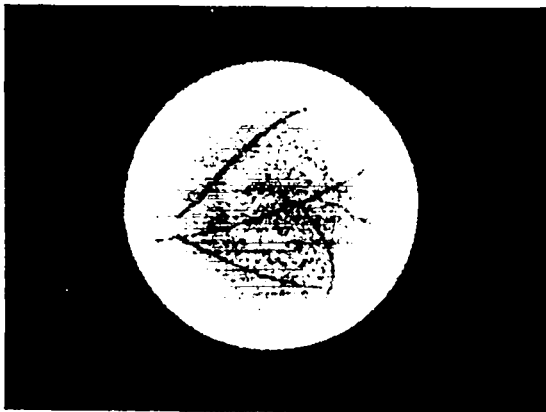
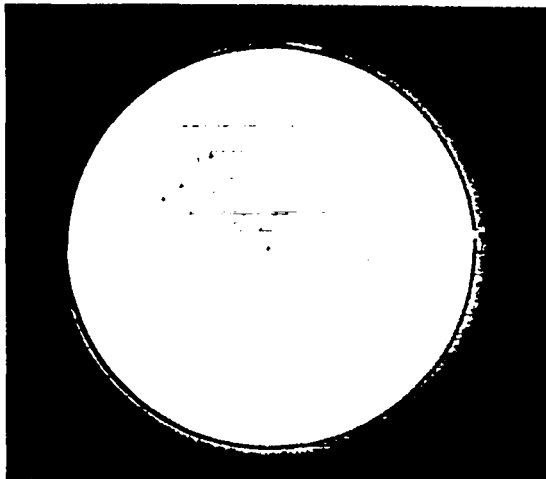


Fig. 6. Typical x-ray microradiographs of: (a) glass microballoon, 100- $\mu\text{m}$ -diam, nonuniform wall; (b) nickel-coated Solacell, 165- $\mu\text{m}$ -diam by 7.5- $\mu\text{m}$ -thick wall; (c) defective nickel-coated Solacell, 175- $\mu\text{m}$ -diam.



(a)



(b)

Fig. 7. Microradiographs of plastic-coated glass microballoons obtained with 2-kV x rays: (a) uniform, 4- $\mu\text{m}$ -thick plastic coating on a cracked, 100- $\mu\text{m}$ -diam glass microballoon; (b) nonuniform plastic coating on a 142- $\mu\text{m}$ -diam glass microballoon; coating is separated from substrate.

6. Nondestructive Fuel Assay. The complexity and slowness of the laser/target interaction experiments makes it mandatory to have the targets completely characterized at the time of the experiment. In particular, we must be sure that the target did indeed contain fuel gas. As a result, we have been developing several methods of nondestructively measuring the deuterium and/or tritium content of the microballoons.

a. X-ray Counting Method. The most convenient (and therefore the most useful) method measures the tritium content of the microballoons by counting the x rays produced when the tritium  $\beta$  particles interact with the walls of the microballoon. When the wall in contact with the tritium is a Ni/Mn/Si-

alloy Solacell, we observe the characteristic  $K_{\alpha}$  x-ray lines of nickel and manganese at 7.5 and 5.9 keV, respectively.

For tritium-filled glass microballoons we see a broad bremsstrahlung x-ray peak at  $\sim 4$  keV for the sodium-borosilicate glass Eccospheres, and a composite bremsstrahlung-calcium  $k_{\alpha}$  peak at  $\sim 3.8$  keV for the soda-lime glass 3M microballoons. (The silicon  $K_{\alpha}$  x-ray at 1.17 keV is not seen in our apparatus because it is absorbed by the window of the x-ray tube.)

The counting system uses 5-cm-diam gas-proportional x-ray tubes filled with 1 atm of xenon ( $\text{CO}_2$  quench), and having 2.5-cm-diam windows of 50- $\mu\text{m}$ -thick Mylar. The microballoons are inserted between two counter tubes placed window-to-window, to increase the counting efficiency. The counters are connected in parallel to a multichannel analyzer through appropriate amplifiers that are balanced by using a  $^{57}\text{Co}$  x-ray source. The gas-proportional counters are very efficient in the energy range of interest and their resolution is more than sufficient to separate the nickel and manganese  $K_{\alpha}$  peaks. Glass microballoons containing less than 2  $\mu\text{Ci}$  of tritium ( $< 0.5$  ng of DT) can be counted with a relative deviation of 2% in 1000-s counting time. The multichannel analyzer output for a bare glass microballoon and for a nickel-coated Solacell are shown in Fig. 8.

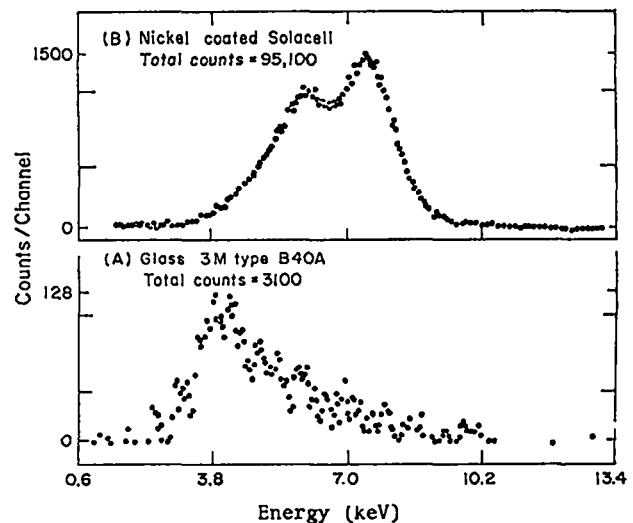


Fig. 8. X-ray counter multichannel analyzer outputs: (a) 3M type B40A glass microballoon, 63- $\mu\text{m}$ -diam by 1.2- $\mu\text{m}$ -thick wall, containing 0.8 ng of tritium; (b) nickel-coated Solacell, 176- $\mu\text{m}$ -diam by 5.7- $\mu\text{m}$ -thick wall, containing 83 ng of tritium.

The primary disadvantage of this method arises because the quantitative x-ray output depends on the materials and thicknesses of the target walls. Therefore, an extensive calibration procedure coupled with a detailed knowledge of the thicknesses of the various layers of the target wall will be required before a quantitative analysis is possible. However, these details are constant in time for any single target so that gas retention half-lives can be measured directly and conveniently with this method by monitoring the count rate of individual microballoons as a function of time. In addition, microspheres that are filled with DT gas to be used as laser targets can be counted very soon after filling to ascertain the initial count rate, which can be related to the amount of gas contained from the knowledge of the fill conditions. Then, when the targets are recounted immediately before mounting in the laser target chamber, the content of DT gas at that time can be calculated from the new count rate and the known initial conditions.

The second disadvantage of the method is its inability to measure the deuterium content. However, this is not too serious a limitation. Except for the 3M microballoons, our practice when loading the targets with DT gas is to keep the spheres at the fill temperature long enough to ensure equilibrium with the ambient gas mixture. Therefore, the initial D/T ratio is known. For metals, the D/T permeability ratio is usually  $\sqrt{3/2}$  (i.e., the smaller deuterium atom permeates  $\sqrt{1.5}$  times faster than the larger tritium atom).<sup>11</sup> A similar D/T permeability ratio for glasses can be estimated from literature data for permeation in fused silica.<sup>12</sup> Therefore, if the tritium loss from a particular target is known, the corresponding deuterium loss can be calculated with reasonable confidence.

#### b. Elastic Scattering (Van de Graaff) Method.

The second nondestructive assay method that is being developed involves bombarding a gas-filled target with protons that are accelerated to  $\sim 16.23$  MeV in LASL's tandem Van de Graaff facility. The deuterons and/or tritons that recoil out of the target as a result of elastic collisions with the bombarding protons are detected and counted. The proton beam is spread out by passing it through a multiple-scattering foil upstream of the target holder, after which a small fraction from the center of this

scattered beam ( $< 10\%$ ) is selected via a 2-mm-diam collimating aperture and used to bathe the target so that a very uniform proton flux is obtained. This collimated proton beam is caught by a Faraday cup downstream of the target and is integrated during the run. This integral and the known areas of collimating aperture and target allow the average proton flux through the target to be calculated which, together with known elastic scattering cross sections, allows us to calculate the deuterium and/or tritium content of the target.

Recent experiments have indicated that we can measure 100-ng quantities of deuterium in nickel-coated Solacells with accuracies of  $\sim 5\%$  in counting times of 30 min, provided that the target walls are not too thick. (5- to 10- $\mu\text{m}$ -thick nickel walls are satisfactory. Thicker nickel walls ( $\sim 20 \mu\text{m}$ ), in particular, cause broadening of the recoil deuteron peak and introduce uncertainties in background corrections.) Similar results are obtained for nickel-coated Solacell targets filled with a 50:50 deuterium-tritium mixture. A glass microballoon containing  $\sim 3$  ng of tritium was also successfully assayed. Indications are that we could measure 1-ng quantities of deuterium or tritium to a statistical accuracy of  $\pm 10\%$  with one-hour counting times.

This method has the advantages of measuring both deuterium and tritium, of being essentially independent of target materials or wall thicknesses, and of requiring no specific calibration. However, the method is rather inconvenient because it requires a rather complex experimental facility whose use must be scheduled well in advance. Its primary usefulness will be in allowing us an independent calibration of other methods, such as the x-ray counting technique.

c.  $D(\gamma, n)$  Reaction Method. The third and final method that is being developed utilizes the  $D(\gamma, n)$  reaction to measure the amount of deuterium contained within a target. In operation, the target to be assayed is placed within a  $^{24}\text{Na}$  source which bombards the target with 2.76-MeV gamma rays to produce 0.25-MeV neutrons. The neutrons are counted in a cylindrical array of 18 polyethylene-moderated  $^3\text{He}$  tubes. A lead-and-tungsten shield assembly is placed between the  $^{24}\text{Na}$  source and the neutron detector to minimize the number of neutrons produced from reaction of the  $\gamma$  rays with the natural deuterium

contained in the polyethylene moderator. The experiments performed to date have demonstrated the feasibility of the method and have provided the data that will allow the optimization of the source-shield-counter system. Current projections indicate that a 300-mCi  $^{24}\text{Na}$  source in a reasonably optimized system will allow 5% counting statistics to be obtained in 1000-s counting time for a sample that contains 100 ng of deuterium. For smaller quantities of deuterium,  $^{24}\text{Na}$  source activities up to 1.5 Ci could be used to increase the sensitivity.

This method suffers from several disadvantages. It measures only deuterium, and the  $^{24}\text{Na}$  source activity must be calibrated frequently against samples of known deuterium content because of the short (15-h) half-life of the  $^{24}\text{Na}$ . In addition, it is somewhat inconvenient because of the necessity of frequent irradiation and handling of the  $^{24}\text{Na}$  source, again because of its short half-life. However, it is independent of target materials and wall thicknesses, and it is substantially less complex than the Van de Graaff method. Here again, the primary usefulness of this method will be in calibrating and verifying the other methods.

A summary of the data obtained in a recent coordinated set of measurements using both the Van de Graaff and the D( $\gamma$ ,n) methods is presented in Table I. In several cases the Van de Graaff method measures more deuterium than we can otherwise account

for. This is believed to be a real effect and we are looking into possible sources of this deuterium.

## 7. Filling, Permeability, and Strength Measurements.

a. Gas Filling. Basic to all of our measurements is the capability of filling microspheres with desired amounts of hydrogen, deuterium, and/or tritium gas. We have fabricated several systems in which the microspheres can be heated to  $\sim 775$  K while being exposed to external pressures of any mixture of the hydrogen isotopes, up to a pressure of 1360 atm. In general, these systems have been fabricated from commercially available high-pressure hardware and fittings, and have used external heat sources to heat the high-pressure tube containing the targets. (We also have under development a system that will allow targets to be exposed to pressures up to 2000 atm at temperatures up to  $\sim 1075$  K. This latter system makes use of a cold-wall pressure vessel with a heated inner vessel to contain the targets.)

The microballoons to be filled with gas are loaded into the apparatus which is then evacuated, charged to pressure with the desired gas, heated to the required filling temperature and held there for an appropriate time, cooled quickly under pressure, and then depressurized. Very little additional gas permeates into the microballoons during cooldown because of the exponential temperature dependence of the permeability. Therefore, the internal pressure

TABLE I  
TARGET GAS CONTENTS

Target Type	Gas Content (ng) and Species		
	Calculated from Fill Conditions	Measured by D( $\gamma$ ,n)	Measured by Van de Graaff
Ni-coated Solacell 314- $\mu\text{m}$ -o.d. by 17- $\mu\text{m}$ -thick wall	845, D <sub>2</sub>	902 $\pm$ 73, D <sub>2</sub>	935 $\pm$ 45, D <sub>2</sub>
Ni-coated Solacell 327- $\mu\text{m}$ -o.d. by 16- $\mu\text{m}$ -thick wall	1000, D <sub>2</sub>	842 $\pm$ 73, D <sub>2</sub>	1038 $\pm$ 55, D <sub>2</sub>
Ni-coated Solacell 173- $\mu\text{m}$ -o.d. by 7- $\mu\text{m}$ -thick wall	156, D <sub>2</sub>	153 $\pm$ 49, D <sub>2</sub>	---
Deuterated polyethylene microsphere	2104, D	Calibration standard; not applicable	2181, D
Ni-coated Solacell 178- $\mu\text{m}$ -o.d. by 7- $\mu\text{m}$ -thick wall	61, D 81, T	----	87.4, D 83.1, T
3M Type B40A glass microballoon 100- $\mu\text{m}$ -o.d. by 1.5- $\mu\text{m}$ -thick wall	6, T 0.1, D	----	5.7, T 2.0, D

in the microballoons at room temperature is that which corresponds to the gas density at the fill conditions.

**b. Permeability Measurements.** Permeabilities were measured initially by filling a large number of pellets under identical conditions and then analyzing their contents as a function of time after filling, using a gas chromatograph. Approximately five pellets were tested for each time interval, to provide good statistics. Recently, all permeability measurements have been made by filling the microballoons with tritium and using the x-ray counting method described above.

We have recently measured the permeabilities of SI Eccospheres in the as-received and heat-treated conditions. These measurements all utilized tritium-filled microballoons and the x-ray counting method. Data obtained for the SI Eccospheres are presented in Fig. 9. The gas-retention half-life,  $t_{1/2}$ , of the as-received microballoons is about one day, which is shorter than expected for a glass of this composition from data reported in the literature.<sup>13</sup>

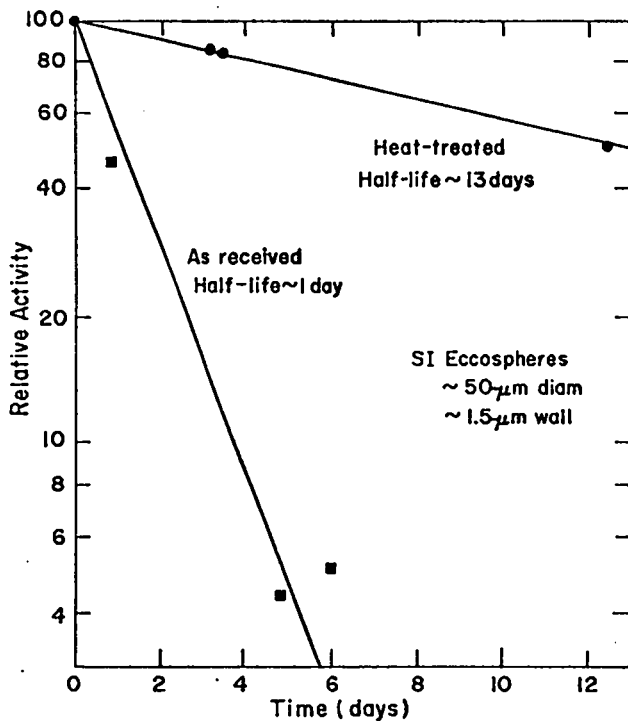


Fig. 9. Tritium gas-retention half-life in glass microballoons measured by x-ray counting method.

A one-day half-life, while not impossible, is inconveniently short to work with. Considering that the SI Eccospheres are made by acid leaching of the IG-101 grade to remove most of the sodium, we suspected that the structure of the SI microballoons was probably rather porous. As a result, we thought that appropriate heat-treatment might well cause the structure to sinter and decrease the permeability. Because it was already necessary to heat treat these microballoons to remove the  $\text{CO}_2$  and  $\text{N}_2$  gases remaining from the manufacturing process, we remeasured the permeability after that heat treatment (20 h at 975 K) and found that the half-life had increased to  $\sim 13$  days, as also indicated in Fig. 9.

We have tried to measure the gas-retention half-life of the 3M glass microballoons by the old method of breaking previously gas-filled spheres and measuring the contents by gas chromatography, and we are measuring some tritium-filled spheres by the x-ray counting technique. The gas-chromatograph data have been obtained out to two months and the decrease in the gas content over that time is within the scatter of the data, which is considerable. The tritium-filled 3M microballoons have been followed for about four months and the decrease in gas content is only slightly more than the scatter of the data. However, a comparison of the gas-filling results obtained for these 3M microballoons with those for the heat-treated SI Eccospheres leads us to conclude that the half-life of the former is at least 30 times longer than that of the latter. As a result, we think the half-life of the 3M, B40A soft-glass microballoons is in excess of one year, and the x-ray counting data are consistent with such a value.

Permeability measurements utilizing the gas chromatograph have been obtained for 20- $\mu\text{m}$ -thick electroless Ni(+P) coatings on  $\sim 250\text{-}\mu\text{m}$ -diam Solacells. The gas permeated out of the pellets at a rate corresponding to a half-life of  $\sim 30$  days. This is a factor of six faster than expected from literature data for the permeability of  $\text{D}_2$  in nickel;<sup>11</sup> we suspect therefore the presence of defects within the coating that provide paths of high permeability.

Permeability measurements have also been obtained for 5- $\mu\text{m}$ -thick electroless Ni(+B) coatings on  $\sim 200\text{-}\mu\text{m}$ -diam Solacells. In this case, the amount of  $\text{D}_2$  contained immediately (i.e., 15 min)

after filling was only  $\sim 240$  to  $270$  atm even for fill pressures (300-K equivalent) as high as  $510$  atm. However, the half-life for subsequent gas loss was about nine days, which agrees reasonably well with the  $\sim 30$ -day half-life observed for the  $20\text{-}\mu\text{m}$ -wall pellets, when normalized for wall thickness. Thus, we conclude that high internal pressures ( $> \sim 270$  atm) in these  $5\text{-}\mu\text{m}$ -wall pellets somehow prop open defects that allow very rapid gas losses; but that at pressures below  $\sim 270$  atm, these gross defects close and the gas is lost only via permeation through the wall as in the thicker-walled pellets.

c. Strength Measurements. Strengths are measured directly by filling appropriate sets of microballoons with gas at successively higher pressures and observing the number of microballoons that burst when the external pressure is released. The strength of the wall material is calculated from the pressure that bursts  $\sim 50\%$  of the microballoons. A new batch of pellets is used at each pressure level because we found some evidence that the metal microballoons were significantly weaker if they were subjected to the filling cycle more than once. The gas content of the microballoons is verified by breaking some of the surviving pellets and analyzing the contents by gas chromatography. We have used deuterium gas exclusively for these tests.

Most of the strength measurements to date have been on the electroless nickel-plated Solacells. Measurements on  $\sim 20\text{-}\mu\text{m}$ -thick deposits of electroless Ni(+P) on  $\sim 250\text{-}\mu\text{m}$ -diam Solacells indicated that  $\sim 50\%$  of the pellets failed by bursting at a wall stress of  $2$  katm.

Similar experiments with  $5\text{-}\mu\text{m}$ -thick electroless Ni(+B) coatings on  $\sim 200\text{-}\mu\text{m}$ -diam Solacells were only partially successful. In this case, we could not burst the pellets even after filling at pressures that corresponded to wall stresses of  $5$  katm, because of the high permeability of these coatings at high pressures as discussed in the preceding section. However, the data from these experiments do allow us to conclude that these  $5\text{-}\mu\text{m}$ -thick Ni(+B) coatings are somewhat stronger than the previously mentioned  $20\text{-}\mu\text{m}$ -thick Ni(+P) coatings. This conclusion is based on the fact that the pressures of  $D_2$  retained in the former ( $240$  to  $270$  atm) correspond to wall stresses of  $2.4$  to  $2.7$  katm and very few pellets are broken, while, as noted above,  $\sim 50\%$  of

the latter broke at a wall stress of  $\sim 2$  katm. Samples are available for strength and permeability measurements of several other thicknesses of nickel coatings made by both the CVD and the electroless deposition techniques. We also have samples of electroless-plated Ni/Co alloys and of CVD molybdenum, tungsten, and rhenium layers. All will be evaluated soon.

#### G. Target Mounting

We have developed techniques for mounting target microspheres on very thin plastic films that can be supported in the target chamber for irradiation by the laser beam. The target holder is made from  $75\text{-}\mu\text{m}$ -thick metal sheet,  $1.5\text{-cm}$ -wide and  $\sim 4\text{-cm}$ -long, with one end rounded on a  $7.5\text{-mm}$  radius. A  $4\text{-mm}$ -diam hole is punched in this metal sheet on the longitudinal center line and  $\sim 7.5$  mm from the rounded end. The plastic support film is attached across the back of this  $4\text{-mm}$ -diam hole and the target microsphere is mounted on the front of the plastic film, approximately in the center of the aperture. (The front of this assembly is defined as the direction from which the laser impinges).

The double-layered plastic film consists of  $\sim 65$  nm of polystyrene backed with  $\sim 30$  nm of cellulose acetate. The target is bonded to the polystyrene surface by heating the assembly to  $\sim 420$  K, which causes the polystyrene to partially melt, become sticky, and bond to the target. The cellulose acetate is not affected at this temperature and therefore provides both structural support for the entire assembly during bonding as well as substantial additional strength at room temperature. This duplex structure was developed because we were not able to bond the target directly to the cellulose acetate and because  $\sim 100\text{-nm}$ -thick, single-layer films of polystyrene were so fragile that very few survived the subsequent handling and coating operations.

The polystyrene films are formed by dipping a glass slide into a  $\sim 1\%$  solution of polystyrene in amyl acetate, and allowing the solution that adheres to the slide after removal to dry and to form a thin, solid polystyrene layer. This solid film is then floated off the glass slide onto a water surface and picked up from above or below with the metal target holder so that it spans the  $4\text{-mm}$ -diam aperture. (The metal holders are precoated with polystyrene by painting with polystyrene solution and allowing the

solvent to evaporate, so as to improve the bond between the metal and the preformed film.) The cellulose acetate films are formed by allowing a drop of cellulose acetate solution (commercial Zapon lacquer diluted 4:1 with amyl acetate) to fall onto water. The drop spreads out to cover almost all available surface and the solvent evaporates to leave a solid cellulose acetate film, floating on the water. The polystyrene film-metal target holder assembly is then placed carefully on top of the floating cellulose acetate film so that the polystyrene surface contacts the cellulose acetate. The two plastic films adhere to each other strongly enough so that the duplex film can be carefully removed from the water surface after the excess cellulose acetate is cut away. The films are allowed to dry thoroughly at room temperature before the targets are mounted.

A major problem encountered with these films was the presence of defects and the tendency to pick up dust particles from the air. Because of this, we obtained a laminar-air-flow clean bench which is used for all of our film-making and mounting operations. This bench enables us to reliably make films that are dust- and defect-free so that we can place the target in any predefined location on the target holder.

We have also mounted targets on thinner plastic films. For experiments in which it is not necessary that the microsphere sit on the surface of the film, single-layer cellulose acetate films are satisfactory. We can then bond the microsphere to the film by dropping the sphere into the cellulose acetate solution floating on the water while the film is still wet (i.e., before the solvent has evaporated). We thus obtain a good bond between the two as the solvent evaporates and the film cures. The microsphere usually protrudes 40% on one side of the film and 60% on the other, but this bulging can be controlled somewhat by controlling both the force with which the microsphere is dropped onto the surface and the time the film has cured before the microsphere is dropped. Target microspheres have thus been mounted on single-layer cellulose acetate films as thin as 20 nm.

#### H. Handling Techniques

We have devoted much time and effort to learning how to handle microspheres, both singly and in batches. In general, the microballoons are so small and

lightweight that their behaviour is controlled predominantly by surface and electrostatic forces, rather than by gravitational forces. Even so, the behaviour of 40- $\mu\text{m}$ -diam glass microballoons with a particle density of  $0.3 \text{ g/cm}^3$  is quite different from that of 200- $\mu\text{m}$ -diam nickel microballoons with a particle density of  $2.1 \text{ g/cm}^3$  so that our handling techniques must accommodate these differences.

1. Handling Individual Microspheres. In general, the microballoons are so fragile that even the most gentle handling with microforceps causes damage. We have therefore developed several other techniques for picking up individual spheres. Most useful is a single hair attached to a dissecting needle or held in a pin vise. The hair is given an electrostatic charge by wiping across an appropriate cloth (polyester clothing is ideal) and then touching the hair lightly to the desired target. Usually, the microsphere will adhere and can be moved to any desired spot. The microsphere can be transferred to a hard surface by gentle wiping or to a liquid by immersion. Human hair works well, especially if straight and dark-colored. The coarseness should be chosen according to the microballoons being manipulated, coarse hair being more effective for the larger, denser targets. For very large, dense targets a fine wire can be used instead of a hair. The bristles of camel's hair brushes are especially useful for the smaller microspheres because these bristles are tapered, with the thin end usually having a diameter of 25- $\mu\text{m}$  or smaller, which allows very delicate manipulations.

A microvacuum pickup is also very useful if two refinements are made: First, the pickup probe must taper upstream from a minimum at the mouth, so that any dust or dirt sucked up into the probe will not plug the gas passage. Second, a source of air at a pressure slightly above atmospheric must be used to blow the microsphere off the pickup probe tip. This is necessary because the electrostatic and/or surface forces are strong enough to hold the sphere otherwise in place indefinitely. A foot-switch-operated solenoid valve is used to connect the pickup probe tip either to the vacuum pump (normal position) or to the compressed-air supply (actuated position). Most useful are pickup probe tips made from glass, by drawing each one down from capillary tubing and carefully breaking off jagged pieces around the mouth to

provide a relatively smooth surface to fit against the microspheres. This transparent tip can be cleaned conveniently by repeatedly sucking up a small amount of appropriate solvent and blowing it out. However, we are also making some probe tips by electrodepositing nickel onto appropriately tapered aluminum mandrels and then etching away the mandrels. In this manner we can easily control both the dimensions and the geometry of the metal tube whose mouth can be machined smooth, but the opacity of the tip is somewhat of a disadvantage. The microvacuum pickup is especially useful when handling the microspheres with mechanical micromanipulators, e.g., mounting the targets on support films.

2. Storage and Retrieval. The larger, heavier, nickel microspheres can be placed individually in small bottles and recovered with good success. However, the transparent glass microballoons with diameters less than 100  $\mu\text{m}$  are so nearly invisible, even under the microscope, that it is virtually impossible to quantitatively recover a small number of these targets that have been placed in a macroscopic container for transportation or storage. Two methods of storage allow us to recover essentially 100% of the microspheres. The first was developed to place and hold the microspheres in a particular location within a regular array for microradiography. The microsphere is transferred to a thin Mylar film (used to support the array during radiography) with a hair or a vacuum pickup and placed in approximately the desired position. Then a microdrop of light oil is added with a second hair. The ball is held in the drop of oil by surface tension and may be pushed with a hair into the exact position. A microsphere so mounted can be subjected to quite severe treatment (such as sending it to another laboratory through the conventional mail) without moving. A 10-by-10 array can be mounted in an area less than 1  $\text{cm}^2$  and radiographed, after which individual spheres can be identified and removed. To remove a sphere from the oil drop, the sphere is pushed with a hair onto an oil-free area of the Mylar film. As the sphere is moved, it leaves a thin trail of oil, depleting the amount of oil adhering to the sphere until the sphere is attracted more strongly to the film of oil on the hair than to the remaining oil on the Mylar, at which point the sphere can be removed from the Mylar. Unfortunately, this method

does leave an oily film on the spheres which must be removed subsequently.

The second method, which utilizes liquids of low density and low surface tension, can also be used for oil removal. Our microballoons are of such low density that many liquids exist that are both denser and will wet the walls of appropriate liquid containers (e.g., glass beakers). Targets placed in such a liquid will float, rising to the highest point in the liquid, which is the meniscus at the edge of the wetted container used to hold the liquid. Thus, all microspheres floating in a beaker of appropriate liquid are quickly confined to a ring at the outside edge of the liquid surface. The curvature of the liquid at this meniscus has a lens effect that magnifies the targets making them much easier to find. A single 50- $\mu\text{m}$ -diam glass microballoon can be washed in a 15-ml beaker half-full of acetone and then located and recovered in a fairly easy and straightforward manner: The ball is removed from the liquid by touching a hair to the surface of the liquid at the edge of the container near the ball; the ball floats to the top of the liquid around the hair and is then pulled up the side of the beaker in the drop of liquid that adheres to the hair. When the ball has been moved above the liquid surface far enough to make retrieval convenient, the hair is pulled away from the beaker wall leaving the ball adhering to the side of the beaker from which it is easily removed with an electrostatically charged hair. This method allows us to store any number of quality-selected and/or gas-filled samples in a beaker and to retrieve any or all at any time by adding an appropriate liquid to the beaker.

3. Batch Recovery. Liquid flotation is also used to recover a batch of microballoons from a container after gas-filling and to collect the microballoons still floating on a liquid surface after a density separation.

The vessels that we use to contain the microballoons during the high-pressure gas-diffusion filling operation are typically small glass capillaries drawn from borosilicate-glass tubing. The bottom end of the capillary is drawn down so that it is almost closed, but a hole slightly smaller than a ball diameter is left in the end while the top end of the capillary is left completely open. The small hole in the bottom prevents the balls from falling through,



but it does allow entrance of an appropriate liquid into the capillary when desired. The microballoons to be gas-filled are loaded, with the aid of a hair, into the open top end of the capillary, and can then be inspected and counted through the glass wall. After gas-filling, the vial can be immersed in a suitable liquid, which flows through the small hole in the bottom of the capillary and floats the spheres out. The balls can then be recovered from the liquid meniscus as discussed above. The liquid also acts both as a cleansing agent to remove oil, dust, and other contaminants, as well as a deagglomerating medium for clumps of microspheres.

We sometimes find it advantageous to perform batchwise density separations of the heavier microballoons in liquid media as discussed in Section F-2 above. When such a separation is carried out in an open beaker, the microballoons that float can be conveniently collected from the surface of the liquid by using an eyedropper partially filled with the separation liquid. If the mouth of this eyedropper is touched to the surface of the liquid in the beaker, a continuous liquid path is available that allows the nearby microballoons to float to the top of the highest liquid surface which is, of course, at the top of the liquid in the eyedropper. The eyedropper mouth can be easily skimmed over the surface of the liquid in the beaker to collect all floating microballoons.

4. General Remarks Regarding Handling. A good binocular microscope and extreme patience are vital for successful handling of the microballoons. Even with our best techniques, the simple act of first finding, and then picking up a particular 50- $\mu$ m-diam glass microballoon and placing it in the desired location, such as on a support film, is a very tedious and time-consuming process. We can put this handling problem into perspective, somewhat, by noting that for targets of the ball-and-disk design, the cumulative time required to make a plastic support film, to retrieve a DT-gas-filled glass microballoon, to mount it on the film, and then to mount and align the mask required for deposition of the disk-type ablator is  $\sim 1.5$  h even for an experienced worker. And this much time is required when everything goes right!!!

#### ACKNOWLEDGMENTS

Our target fabrication program has utilized, and benefited from, the capabilities and expertise of scientists, engineers, and technicians in at least 27 different LASL groups situated in nine different divisions, as well as those of the members of the Advanced Engineering Department at Bendix, Kansas City Division. And this does not count the support we receive from within the Laser Division, itself.

A major share of our target-fabrication development support has come from Group CMB-6, with a large fraction of the effort within this group coming from the powder metallurgy section. Bob Riley, Hack Sheinberg, Bill McCreary, and Dick Honnell, with the help of Barry Barthell, Dave Carroll, John Kostacopoulos, John Magnuson, Bud Richerson, and Larry Tellier have contributed in many areas of target fabrication including microballoon sizing, quality selection and characterization, metal deposition by PVD, CVD, and sputtering, heat-treatment, LiD microsphere fabrication, and free-standing metal microballoon fabrication.

Also in CMB-6, Bill Powell and Jim Glass of the electrochemistry section have contributed, primarily in the areas of electro- and electroless plating of microspheres. Gary Simonsic and Steve Newfield of the plastics section have contributed in the areas of plastic coating of microballoons, disk ablator deposition, and solid plastic microsphere fabrication. In addition, we have also benefited from the skills and knowledge of the members of the Ceramics, Foundry, and Physical Metallurgy sections as well as those of Jim Taub and Don Sandstrom, the group leader and alternate group leader, respectively, of CMB-6.

In Group CMB-3, Dean Carstens has contributed in the areas of gas-filling techniques, content analysis, and strength measurement of microballoons; target mounting and disk ablator deposition and D/T exchange reactions with LiD. Dick Briesmeister and Joe Nasise also helped with the D/T exchange work. Also in CMB-3, Jim Anderson has willingly shared with us his knowledge of tritium systems in general and LiD/LiT in particular.

The members of Group CMB-1 have performed many chemical and other types of analyses for us, and Maynard Smith, Nancy Koski, and Joe Bubernak have been especially helpful. In Group CMB-8, Paul Wagner, Lyle Wahman, and Ralph White have run some pyrocarbon coating experiments for us.

All of our cryogenic target development is being carried out in Group Q-26 by Ed Grilly and Steve Sydoriak with the help of many others both within and outside of Q-26.

Max Winkler, Tom Gregory, and Ron London of Group M-1 have contributed in the areas of x-ray microradiography, scanning-electron microscopy, and thin plastic-film fabrication.

The members of Group WX-5 have helped us with high-pressure gas-handling problems in general, and tritium handling and target filling in particular. Don Coffin, Dick Maltrud, Al Manthei, Bob Stoll, and George Whitehead have been especially helpful.

The  $D(\gamma, n)$  method for nondestructive assay of the  $D_2$  content of microballoons was proposed by Henry Atwater and John Caldwell of Group A-1 and was developed by them with the help of Tony Hyder, also of Group A-1. The elastic scattering method for the nondestructive assay of DT was proposed by Bill Jarmie of P-DOR and developed by him with the help of Paul Lavoie of P-DOR and Louis Morrison and the Van de Graaff staff of Group P-9. Judy Gursky of Group P-12 also helped by developing methods of mounting the microsphere targets for the Van de Graaff experiments.

In addition to the foregoing, George Auchampaugh and Darrell Drake of Group P-3 performed some experiments to evaluate the feasibility of another DT assay method involving the detection of neutrons produced by bombarding the target microspheres with deuterons or tritons. Merle Bunker and Bill Starner in P-2 helped us evaluate the usefulness of the x-ray counting method of measuring tritium contained in microballoons. Others in P-2 have contributed by irradiating the  $Na_2CO_3$  sources used in the  $D(\gamma, n)$  assay method as well as by irradiating several other samples for us.

At Bendix, Kansas City Division, a laser-target project team consisting of Jerry Havenhill, Dan Stoltz, Dave Fossey, Chuck Stimetz, Larry Lantz, Jerry Keuhnle, and Maurice Smith has made significant contributions in many areas of target fabrication. These include plastic coating of microspheres; metal coating by electro- and electroless plating techniques; chemical vapor deposition; and microballoon quality selection, characterization, and modification.

In addition to the above, one or more members of LASL Groups A-1; CMB-7; E-4; ENG-6; H-5; SD-1, -3, -4, -5, and -6; WX-1; and WX-2 have helped, and/or are helping, us out of one bind or another in numerous ways. We also want to note that many members of our own group, L-4, have helped us in this effort, especially Gordon Hoffman with metallography, Dave Kohler with interferometry, and Fred Young with the Van de Graaff experiments.

One of the most satisfying aspects of our work in laser target fabrication has been the realization and utilization of the fact that virtually the entire laboratory staff is genuinely interested in our program to develop laser fusion and is very willing to help us solve the problems that we encountered while trying to fabricate these ridiculous little balls we call laser targets. Whatever successes we have had, and will have in the future, will result in large measure from this incredibly broad base of support that we have been able to call upon.

#### REFERENCES

1. Keith Boyer, Los Alamos Scientific Laboratory, private communication, Jan. 1974.
2. R. L. Morse, Los Alamos Scientific Laboratory, private communication, Jan. 1974.
3. D. E. Wood, "Some Principles of Neutron Activation," Kaman Nuclear Co. report KN-68-71 (February 1968).
4. G. O. Mallory, *Plating* (April 1971) p. 319.
5. K. M. Gorbunova et al., *J. Electrochem. Soc.* 120, 613 (1973).
6. D. Fossey and M. L. Smith, The Bendix Corporation, Kansas City Division, private communication, August 1973.
7. R. J. Bard, Los Alamos Scientific Laboratory, private communication (1973).
8. P. M. S. Jones and R. J. Gibson, *Nucl. Mats.* 21, 353 (1967).
9. T. Elleman, Gulf General Atomic, San Diego, CA and North Carolina State University, private communication (1973).
10. R. J. Roark, Formulas for Stress and Strain, 4th Ed (McGraw-Hill, New York, 1965).
11. M. R. Louthan, J. A. Donovan, and G. R. Caskey, "Isotopic Effects on Hydrogen Transport in Nickel," submitted to Scripta Met.

12. R. W. Lee, R. C. Frank, and D. E. Swets, J. Chem. Phys. 36, 1062 (1962).
13. (a) L. C. Walters, J. Am. Ceramic Soc. 53, 288 (1970).  
(b) W. G. Perkins and D. R. Begeal, J. Chem. Phys. 54 (1971).  
(c) J. L. Barton and M. J. Morain, J. Non-Crystalline Solids, 3, 115 (1970).  
(d) H. M. Laska, R. H. Doremus, and P. J. Jorgensen, J. Chem. Phys. 50, 135 (1969).

Printed in the United States of America. Available from  
 National Technical Information Service  
 US Department of Commerce  
 5285 Port Royal Road  
 Springfield, VA 22161

Microfiche \$3.00

001-025	4.00	126-150	7.25	251-275	10.75	376-400	13.00	501-525	15.25
026-050	4.50	151-175	8.00	276-300	11.00	401-425	13.25	526-550	15.50
051-075	5.25	176-200	9.00	301-325	11.75	426-450	14.00	551-575	16.25
076-100	6.00	201-225	9.25	326-350	12.00	451-475	14.50	576-600	16.50
101-125	6.50	226-250	9.50	351-375	12.50	476-500	15.00	601-up	

Note: Add \$2.50 for each additional 100-page increment from 601 pages up.